Optical properties versus growth conditions of CdTe submonolayers inserted in ZnTe quantum wells

Vincent Calvo
Groupe d'Etude des Semiconducteurs, CNRS, Université Montpellier II, Case Courrier 074, 34095 Montpellier Cedex 5, France

Noël Magnea
CEA Grenoble, Département de Recherche Fondamentale sur la Matière Condensée/SP2M, 17 avenue des Martyrs, 38054 Grenoble, France

Thierry Taliercio, Pierre Lefebvre, Jacques Allègre, and Henry Mathieu
Groupe d'Etude des Semiconducteurs, CNRS, Université Montpellier II, Case Courrier 074, 34095 Montpellier Cedex 5, France
(Received 15 April 1998)

Standard and piezomodulated optical spectroscopy is performed on ZnTe quantum wells embedding integer and fractional monolayers of CdTe. The samples, grown in a molecular-beam-epitaxy setup on the (001) surface of ZnTe substrates, all basically consist of 120-ML-wide ZnTe/(Zn,Mg)Te quantum wells, and some of them contain five equally spaced full or half-monolayers of CdTe, producing monomolecular islands of CdTe ''buried'' in the wide host ZnTe well. The latter behave as efficient recombination centers for excitons. In order to change the size and the configuration of the islands, various growth parameters have been changed between the different samples, e.g., the growth process (molecular-beam epitaxy of binaries or ternaries, or atomic-layer epitaxy) or the temperature. From spectroscopic measurements, the influence of these parameters is analyzed in detail, in terms of the size of the islands and of their in-plane spacing, or of the vertical correlation between these islands. The internal strain state of the CdTe insertions and the overall photoluminescence efficiency are also studied versus growth conditions. [S0163-1829(98)01047-9]

I. INTRODUCTION

A variety of techniques have been tried in the past decade for improving the properties of semiconductor light-emitting and light-detecting devices. In most cases, an important amplification of optical phenomena has been produced by the reduction of dimensionality, leading to the growth of quantum wells (QW's) and superlattices (quasi-2D), quantum wires (quasi-1D), and quantum dots (quasi-0D). The fabrication of high-quality QW's and superlattices has been achieved on almost all kinds of semiconductors by the development of advanced epitaxial growth techniques. Concerning structures with lower dimensionalities, there is still an active research aiming at the development of methods which would avoid numerous processing stages and would provide reliable, reproducible, low-dimensional objects. In the past few years, a considerable amount of interest has been focused, in particular, on deposition procedures which allow for the self-organized growth of nanoislands.[1–4] For example, the so-called Stranski-Krastanov growth mode of highly lattice-mismatched crystals has been exploited to produce flat pyramids of a narrow-gap semiconductor, embedded in a matrix made of a wider gap material. Another approach has also been tried, both for III-V (Refs. 5–8) and II-VI (Refs. 9–14) semiconductors, i.e., the insertion of fractional monolayers of the narrow-gap material, acting as efficient radiative recombination centers, within the wider-gap host. Recently, such growth has allowed to improve the operating conditions of some lasers based on CdSe and ZnMgSSe,[15] which currently suffer from the competition with III-nitride-based devices.

In recent works, we have obtained indications of self-organized growth mechanisms when embedding either ZnTe half-monolayers in CdTe QW's (Refs. 11–13) or half-monolayers of CdTe in ZnTe matrices.[14] Structural characterizations by reflection high-energy electron diffraction (RHEED), x-ray diffraction, and, above all, scanning tunneling microscopy (STM) (Ref. 16) have shown that such growth of less than one monolayer always produces a coverage of the surface by islands having one monolayer in height and various lateral sizes, depending on the details of the growth.

The purpose of this paper is to give detailed insight into the correlation between the thermodynamical conditions of deposition of such fractional monolayers and their optical properties. The techniques used for this investigation are all based on low-temperature optical spectroscopy: photoluminescence (PL) and both standard and piezomodulated reflectivity. From our measurements, we obtain valuable information on several important issues such as island sizes, strain states, and the efficiency of radiative emission from these objects. We also demonstrate the difficulty of an accurate theoretical treatment by the usual envelope-function calculations in this context.

II. SAMPLES AND EXPERIMENTAL RESULTS

Figure 1 shows the typical structure of our samples, which have all been grown by molecular-beam epitaxy (MBE) on

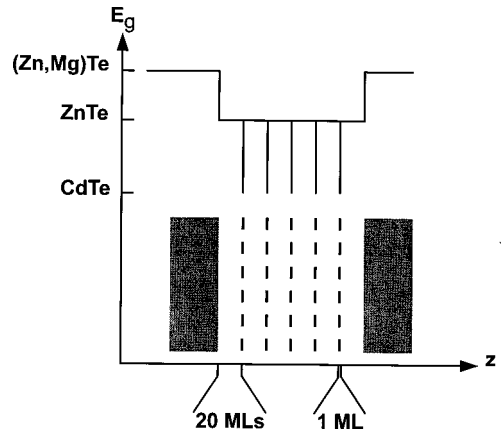

FIG. 1. Sketch of the real-space geometry (bottom) and band-gap profile (top) along the (001) growth axis of our samples. Gray and white areas represent the (Zn,Mg)Te pseudoalloy barriers and the 120-ML-wide ZnTe quantum well, respectively. Dashed bold lines show the position of the various narrow-gap insertions.

the (001) surface of ZnTe substrates: two (Zn,Mg)Te barriers (gray areas) surround a ZnTe QW (white area), which has a nominal thickness of 120 monolayers (ML) i.e., approximately 38 nm. More precisely, the barriers are made of ZnTe/MgTe (samples 0 and 2–5) or $ZnTe/Zn_{0.5}Mg_{0.5}Te$ (sample 1) superlattices with ultrashort periods (e.g., 1 MgTe ML/4 ZnTe ML). The Mg-rich layers of these superlattices are biaxially compressed by lattice-matching to the substrate, inducing a splitting of light- (lh) and heavy-hole (hh) states which adds to that provoked by confinement effects. The ZnTe well is *a priori* unstrained, since the barrier thickness lies below the critical thickness in this system. Bold dashed lines in Fig. 1 show the positions of the five monomolecular inserts, if any, constituting full or half-monolayers of CdTe and deposited, every 20 ML of ZnTe, under various thermodynamical conditions. The top of Fig. 1 displays the variation of band gap versus position along the growth (z) axis.

Figure 2 displays the reflectivity (a) and PL (b) spectra obtained from samples 0–5 at pumped liquid helium temperature. No particular care has been taken concerning excitation densities and wavelengths in PL experiments. The average power density used here is of the order of ~ 100 W cm^{-2}, whereas all visible lines of an ionized Ar laser (principally the 514 and 488 nm lines) have been used. Table I summarizes the growth parameters and experimental results obtained from samples 0–5. We will comment on these results below, together with the description of the growth conditions and the specificity of each sample, for clarity.

Sample 0 is simply the ''empty'' ZnTe quantum well. The corresponding reflectance spectrum shows a strong feature near 2.38 eV. This feature is common to all our samples and corresponds to the excitonic gap of the ZnTe substrate. Also characteristic of all the substrates are the PL lines at 2.378, 2.375, and 2.374 eV and their LO-phonon replica in the 2.348–2.352 eV range, which correspond, respectively, to the recombination of donor-bound excitons (first line) and acceptor-bound excitons (second and third line). Sample 0 exhibits additional reflectivity and PL features which are attributed to the so-called center-of-mass quantization (CMQ) of lh and hh excitons[14,17,18] in the ZnTe QW. This observa-

TABLE I. Growth characteristics of the samples and experimental transition energies. H_B and L_B represent the hh and lh excitons in the ZnMgTe barriers as measured by reflectivity at $T=2$ K. Transitions $e1h1$ and $e1l1$ denote the energies of the hh and lh excitons trapped on the various CdTe inserts.

Insert growth conditions					Excitons trapped on the inserts		Excitons of the barriers	
Sample	Nature	Technique	Temperature (°C)	Nominal barrier composition	$e1$-$h1$ (eV)	$e1$-$l1$ (eV)	H_B (eV)	L_B (eV)
0	None	MBE	330	4 ML ZnTe/ 1 ML $Zn_{0.5}Mg_{0.5}Te$			2.428	2.444
1	5 full CdTe monolayers	MBE	330	4 ML ZnTe/ 1 ML MgTe	2.344	2.358	2.442	2.463
2	5 $Cd_{0.5}Zn_{0.5}Te$ monolayers	MBE	330	4 ML ZnTe/ 1 ML MgTe	2.371	2.376	2.430	2.445
3	5 half CdTe monolayers	MBE	330	4 ML ZnTe/ 1 ML MgTe	2.359	2.367	2.462	2.489
4	5 half CdTe monolayers	ALE	330	4 ML ZnTe/ 1 ML MgTe	2.366	2.371	2.466	2.495
5	5 half CdTe monolayers	MBE	230	4 ML ZnTe/ 1 ML MgTe	2.344 2.350	2.355 2.358	2.428	2.445
6	None	MBE	330	4 ML ZnTe/ 1 ML MgTe			2.456	2.482
7	5 half CdTe monolayers	MBE	330	4 ML ZnTe/ 1 ML MgTe	2.359	2.366	2.459	2.485
8	5 inserts of $2x$(1/2CdTe +1/2ZnTe)	MBE	330	4 ML ZnTe/ 1 ML MgTe	2.340	2.355	2.457	2.484

tion is favored by the ZnTe well width which equals approximately four times the exciton Bohr diameter.

Sample 1 contains full CdTe ML deposited by classical MBE, i.e., by opening the shutters of both Cd and Te effusion cells simultaneously, the amount of exactly 1 ML being controlled by the deposition time and by RHEED pattern oscillations. For all the samples described in this paper, the amount of CdTe has been controlled *in situ* by this method and crossed-checked by subsequent x-ray diffraction. The thicknesses measured by the latter technique always differ by less than 10% from those determined by RHEED measurements.

The reflectivity spectrum reveals two additional structures at 2.344 and 2.358 eV, which correspond to the hh and lh ground exciton states, ''confined'' in the CdTe ultrathin QW's. We prefer to say that these excitons are trapped on the CdTe inserts which act as shallow isoelectronic traps, since their energies are less than 40 meV below the excitonic gap of ZnTe, to be compared to the excitonic gap of CdTe: 1.594 eV. The trapped excitons of this kind which are studied throughout this paper have thus probably a quasitridimensional relative motion of electrons and holes and thus assume almost the same binding energy as in bulk ZnTe. Anyway, their centers of mass are pinned onto the inserts. The fundamental hh exciton gives rise to a weakly Stokes-shifted PL line ($\sim$0.5 meV between the PL maximum and the reflectance minimum), with a half-width at half-maximum (HWHM) of 3 meV. The lh exciton can also be observed by amplification of the PL spectrum in this region. The features of the CMQ observed in sample 0 are no longer observed here, which corresponds to the fact that excitons cannot freely cross the entire ZnTe QW without meeting CdTe layers. Consequently, the confinement of exciton polaritons in the wide ZnTe well can only manifest itself by extremely weak oscillations of the reflectivity, corresponding to ''resonant'' states, above 2.38 eV. But no PL signal is measured from these states because the carriers are all trapped by CdTe inserts.

For sample 2 all three cells of Cd, Zn, and Te have been opened during the growth of the inserts, yielding five full ML of $Cd_{0.5}Zn_{0.5}Te$. In other words, the conditions have been made such that each insertion contains equal proportions of Cd and Zn atoms, randomly distributed in the layer plane. The reflectance features of the hh and lh trapped excitons appear as doublets near 2.372 and 2.377 eV, respectively, i.e., much closer to the ZnTe gap than for sample 1. The presence of double structures has been assigned recently[19] to the appearance of negatively charged excitons, denoted X^-, similar to those already observed in many instances[20–23] in wider CdTe and GaAs QW's under artificial or nonintentional excess of electrons. These excitonic complexes correspond to the low-energy components of the reflectivity and PL features (see the PL shoulder at 2.37 eV). Arguments in favor of this assignment as well as a detailed study of X^- complexes in our samples will be published elsewhere. Note the small HWHM of the PL line: $\sim$0.9 meV.

The situations of these first three samples are, to some extent, rather classical since only integer numbers of monolayers have been deposited, inducing no intentional in-plane morphology. For samples 3–5, the overall Cd and Zn compositions of the inserts are the same as in sample 2, but the deposition techniques are completely different, with important consequences on the in-plane repartition of Cd and Zn atoms, and on optical properties.

For growing the inserts in sample 3, we have set the conditions necessary for the bidimensional growth of CdTe on ZnTe but we have done this only for the time required for filling half a plane, the other half being filled with ZnTe. This has been repeated five times, separated by the growth of 20 ML ZnTe spacers. The expected morphology, in this case, is made of relatively wide, flat (1 ML in height) islands of CdTe embedded in the host ZnTe QW. STM has confirmed recently[16] that the islands grown by such ''classical'' MBE have in-plane sizes in the range of 20–30 nm, i.e., four to six times the exciton Bohr radius in ZnTe. The optical spectra of sample 3 exhibit two independent sets of features: (i) those due to hh and lh excitons trapped on CdTe inserts, at 2.358 and 2.367 eV; (ii) the multiple structures, above 2.38 eV, due to the CMQ of excitons in the wide ZnTe QW.[14,17] This specific behavior, together with time-resolved PL results, has been interpreted in a previous work[14] as a strong indication that the CdTe islands are quite a bit larger than the Bohr diameter of excitons ($\sim$10 nm), with in-plane spacing of the same order of magnitude, and that there exists some vertical correlation of the islands of successive inserts. In other words, the wide flat islands of the five different inserts are vertically stacked ''on top of each other,'' leaving between them wide ''tubes'' of pure ZnTe, in which the excitons can coherently establish their CMQ pattern. The mechanism leading to such a vertical stacking is probably related in a complex way to the strain and size of the buried islands and to the thickness of the spacers between the inserted planes.[24] Indeed, it has been shown recently that both vertical correlation or anticorrelation could occur, depending on the geometric parameters of the structure.

From recent investigations by STM,[16] we can also expect some regularity of island sizes and of their distribution in the plane, if not a quasiperiodicity. Moreover, the shape of these islands is square or rectangular, with edges parallel to the (100) and (010) directions of the plane. The same shapes are observed for islands grown by atomic-layer epitaxy (ALE), such as sample 4, but lateral sizes appeared smaller, in the range of 5 nm.

The ALE method basically consists in opening the shutters of the Cd and Te sources *one at a time*. This has proved[25,26] to induce particular surface reconstructions during the deposition of single species and to allow for the observation of a subperiodicity of RHEED oscillations. The latter reveals two steps within the deposition of a single ML, each one corresponding to the adsorption of half the total quantity of cadmium atoms of the full ML. This property has been exploited here in order to control the deposition of particular half-monolayers of CdTe. Due to the use of fluxes containing single species, the mechanism of adsorption by ALE is very different from that obtained by classical MBE. Indeed, the latter produces the bidimensional progression of randomly distributed steps which exist on the deposition surface, by adjunction of Cd-Te dimers. On the other hand, the absence of Te during one step of the deposition by ALE of half ML rather leads to a quasiperfect wetting of the entire surface by Cd atoms.[25,26] Then, when Te atoms are sent onto

the sample, small CdTe islands tend to constitute at some nucleation sites, by ''stealing'' Cd atoms from their vicinity, leaving Te-rich surfaces, less high by 1 ML, between them. This technique is known to allow for an excellent control of the quantity of Cd adatoms deposited but provides smaller CdTe islands than the MBE technique.[16] The possibility to control the in-plane size being one of our interests, we have also investigated the effect of changing the growth temperature.

Sample 5 gives an illustration of our attempt to grow insertions similar to those in sample 3, i.e., by classical MBE, but using much lower temperature (230 °C instead of 330 °C). This was expected to reduce the surface mobility of adatoms, inducing smaller islands than in sample 2. In fact, the result, shown in Fig. 2, is quite unexpected: we observe an intricate series of transitions, some of which are attributed to X^- complexes, involving both hh and lh excitons, as demonstrated and discussed below.

III. THEORETICAL CONSIDERATIONS

Calculations based on the envelope-function approximation and the formalism of deformation potentials have been used and refined successfully in the past decade to describe electronic and excitonic states in a large variety of strained-layer QW's and superlattices. More recently, this approach has been applied to objects of lower dimensionality, such as quantum wires,[27] quasispherical nanocrystals,[28,29] flat pyramids on wetting layers,[30] or ZnTe monomolecular inserts in CdTe QW's.[13] However, there exists a controversy in the current literature concerning the accuracy of this method compared, for instance, to pseudopotential[31,32] or tight-binding[33] calculations, in particular for systems operating a strong real-space localization of carriers. It is not our purpose to enter into this debate, but we remark that the theoretical treatment of the present experimental cases is a very difficult task. Indeed, our fractional insertions of CdTe may be regarded as a special kind of isoelectronic δ doping within the ZnTe QW rather than as CdTe QW's. In fact, the description of our samples with a reasonable accuracy by envelope-function calculations is difficult. After several attempts, we have found out that this is not only due to the lack of knowledge of some parameters such as band offsets, strain states, lateral sizes, or real compositions and thicknesses of the layers. In fact, the concepts of potential well depths and widths for electrons, hh's, and lh's are impossible to apply as such here. Moreover, the usual notion of biaxial lattice-mismatch strain does not stand, except in the cases of samples 1 and 2.

We believe that a microscopic treatment of these objects is still desired. This modeling should consider the problem of substitutional Cd atoms in the Zn sublattice, assuming various geometries and lattice relaxations.

Anyway, we can describe and discuss a few trends that we have extracted from our attempts. We have used a classical transfer-matrix algorithm to describe our multilayered systems. We found that the largest source of inaccuracy of our calculations is the value of the ''exact'' well width to be used in this procedure. For example, in the case of sample 1, which is *a priori* the simplest sample (full ML, biaxial strain), we calculate the fundamental $e1h1$ and $e1l1$ excitonic transitions ~13 meV below the experimental values, with a correct description of their energy difference of 12 meV. This is really an important point since the band lineup for the $e1h1$ transition is type I, whereas it is type II for the $e1l1$ transition, under the assumed conditions of ''chemi-

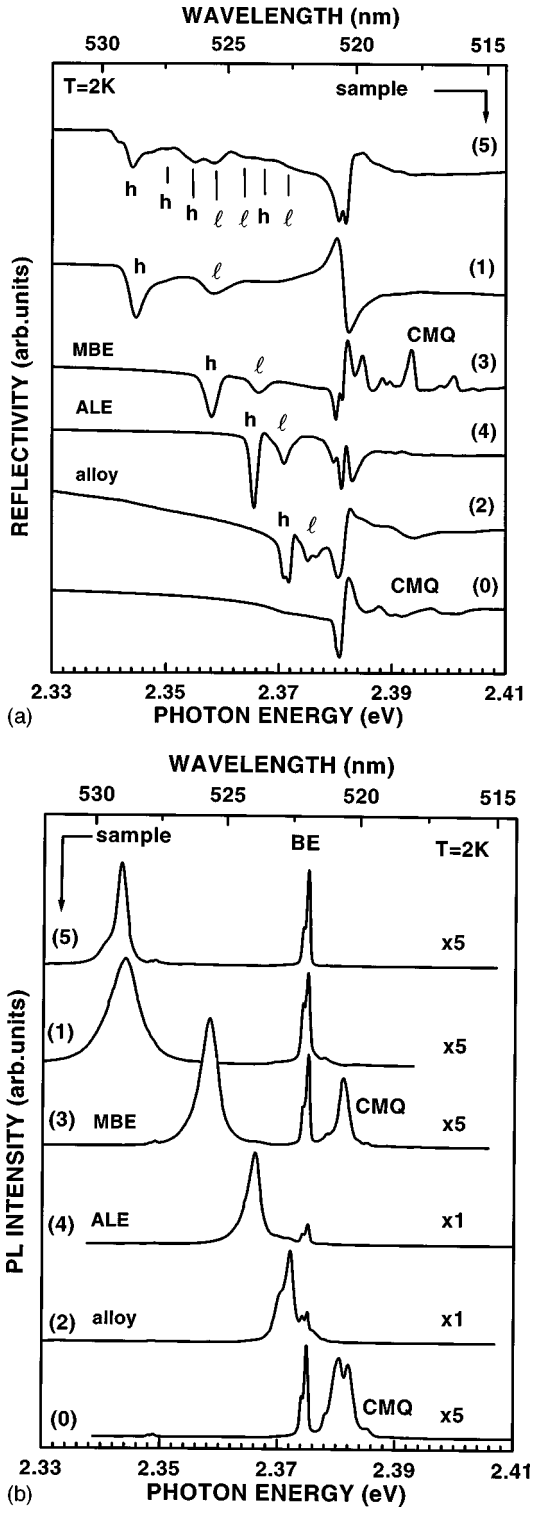

FIG. 2. Optical spectra taken at $T=2$ K for samples 0–5. (a) Reflectivity; (b) photoluminescence. Symbols ''*h*'' and ''*l*'' indicate the positions of hh and lh excitonic transitions, respectively, as deduced from piezoreflectivity experiments. The spectra have been ordered from top to bottom by increasing energies of the ground hh exciton.

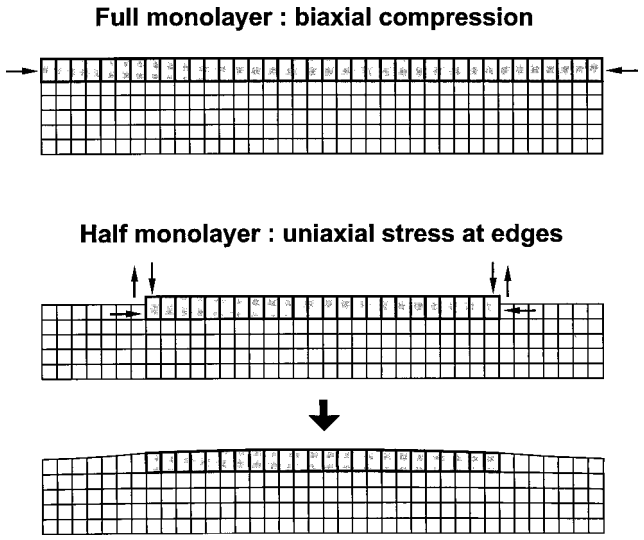

FIG. 3. Sketch of the strains undergone by CdTe inserts in the case of full monolayers (biaxial strain—top of the figure) and of half monolayers, producing flat islands (additional uniaxial strain at edges—bottom of the figure).

cal'' valence-band offset ($\Delta E_v = 0.1\,\Delta E_g$) and of energy shift induced by lattice matching of CdTe on the ZnTe substrate. In the case of sample 2 ($Cd_{0.5}Zn_{0.5}Te$ ML), we have considered inserts made of a virtual crystal, in total biaxial compression by lattice-matching on ZnTe. By using Vegard's law for all the pertinent parameters of the $Cd_{0.5}Zn_{0.5}Te$ alloy, we have also calculated both transitions $\sim$13 meV below their experimental values, again with the correct spacing of 6 meV. Thus, we may consider that our calculations suffer from a slight overestimation of the well widths (of course, a slight uncertainty on the alloy composition cannot be discarded for sample 2). In the following, we discuss our results a bit further, in terms of island sizes, ordering, and strains.

IV. DISCUSSION

First, let us compare samples 1 and 3. From our observations, we understand that the islands in sample 3 are very wide, compared to the exciton Bohr diameter, separated by ZnTe zones of the same dimensions so that the CMQ can take place. In fact, the CdTe islands in sample 3 are almost wide enough to be ''seen'' as entire monolayers by the excitons trapped on them. In other words, there should be no particular lateral confinement effect here, at least in the usual sense. The essential difference between sample 1 and sample 3 must be the strain state. We will try to give a picture of what occurs in the two cases, corresponding to the sketch in Fig. 3.

For sample 1, we face the classical situation of pseudomorphic, biaxially strained monolayers. The electronic and excitonic energies of the system account for both confinement effects and for the biaxial strain. Now, in the case of the inserts in sample 3, specific effects are expected at the boundaries between the islands and the surrounding ZnTe. There has to be a displacement of Cd atoms, corresponding to an additional compression of Cd-Te bonds along the growth axis, due to the lattice matching with ZnTe, at least at the edges of the islands. This assumption is consistent with the blueshift of the ground hh and lh excitons from sample 1 to sample 3, and with the fact that they become closer to each other, due to the partial compensation of the splitting induced by the shear component of the biaxial stress by that induced by the additional vertical uniaxial stress.

We have modeled an ideal situation where an equilibrium is reached by the system with the vertical lattice parameter a_z constant over the whole surface of the islanded layer, i.e., the same value for both CdTe islands and ZnTe ''lakes,'' which occupy equal total surfaces. This can be made by minimizing the total elastic energy stocked in the system versus a_z, just like what is usually done for free-standing superlattices, versus $a_\perp$. Then, the strain and stress undergone by each of the two materials present can be evaluated. Since the symmetry of the deformation is both biaxial in the (001) plane and uniaxial along the (001) axis, the lh and hh valence-band states are not mixed by the strain. We can use a model similar to that used for biaxially strained layers, but we just have to change the potential well depths accordingly with the results of the deformation potential formalism.[34] We shall not go into the details of the calculation. The main result in the present case is that the ZnTe, which is a stiffer material, only undergoes a small vertical tension. On the other hand, the CdTe layer is almost hydrostatically compressed. The stress tensor is found to be of the form

$$\vec{X}_{001} = \begin{bmatrix} X & 0 & 0 \\ 0 & X & 0 \\ 0 & 0 & Z \end{bmatrix} \tag{1}$$

with $X \sim 15$ kbar and $Z \sim 12$ kbar. The consequence of this huge deformation of CdTe is that the energies of conduction- and valence-band states of CdTe are increased. Consequently, compared to the case of sample 1, the potential well depth for electrons is reduced from $\sim$600 to $\sim$300 meV, and both $e1h1$ and $e1l1$ transitions now have a type-II band lineup. The theoretical result is that both transitions are predicted to lie at $\sim$2.365 eV. Considering that our calculation underestimates transition energies by $\sim$13 meV (see above), we find that the hypothesis of the uniform lattice parameter across the plane cannot correspond to the cases of samples 3 and 4.

In fact, there are probably significant variations of a_z across the layer plane. We propose the picture sketched in Fig. 3: The situation at the edges of the islands is probably quite close to that described in the preceding paragraph, while the center of the islands would face a more classical situation of biaxial compression. Then a gradient of potential energy would exist between the edges and the middle of the islands (of the order of 300 meV for electrons, from the above remark). This should operate a particular kind of confinement of the carriers in the plane of the islands, leading to the blueshift of the optical transitions, compared to the model case of sample 1.

This picture is particularly well suited for explaining some particular points that had already been raised in previous papers:[14,17] (i) the fact that the CMQ features are much clearer in sample 3 than in sample 0; (ii) the fact that the

decay time of the PL from the CMQ states is of ~250 ps whereas the *lower-lying* PL from the inserts is much faster ($\tau \sim 70$ ps); (iii) the fact that the fundamental transition of the CMQ in the wide ZnTe well involves lh excitons, instead of hh excitons, as for sample 0. Indeed, the presence of an almost hydrostatic deformation at the edges of the CdTe islands induces potential barriers for both types of holes, as already noticed. Then, the excitons lying in the ZnTe vertical ''tubes'' in between the stacked CdTe islands are prevented from falling into the islands by these barriers. This explains why their higher-energy recombination can decay more slowly than the $e1h1$ and may also explain the intensity of CMQ features since the excitons are really maintained within the tubes by potential barriers. Moreover, the slight uniaxial deformation of ZnTe between the islands may explain the redshift of the ground lh exciton.

Now considering sample 4, we remark that the hh and lh excitons are even more blueshifted than for sample 3, which we attribute to smaller islands, leading to a less inhomogeneous deformation of a_z across the islands. The boundary effects described above for wider islands do not disappear totally at the center of the inserts. We must then consider, in this case, more substantial lateral confinement effects, accompanied by a strong in-plane coupling between all the islands, by tunneling across narrower ZnTe ''barriers.''

Thus, the inserts in sample 4 may be seen as very small CdTe islands, i.e., a special kind of ordered $Cd_{0.5}Zn_{0.5}Te$ alloy. This ordering explains the lower exciton energies in this sample than those in sample 2, where the inserts are made of disordered $Cd_{0.5}Zn_{0.5}Te$. Figure 2(b) clearly shows, also, that under comparable excitation conditions, the strongest PL intensity from the CdTe inserts is obtained for sample 4. We interpret this result as a consequence of this ordering (periodicity) and of the tunnel effect which occurs between CdTe islands both in the plane of the inserts and along the growth axis, between the inserts. This resonant coupling between the ''island states'' induces the delocalization of the envelope functions of the carriers across the entire ZnTe layer containing the inserts, which may be viewed as a kind of three-dimensional superlattice, or superalloy. This explains why the loss of carriers towards nonradiative channels is reduced, increasing the efficiency of the PL.

To support this picture, let us consider what occurs when we purposely destroy the in-plane island ordering and the vertical correlation between them. This is the case of sample 5, which was obtained by using a low growth temperature. The piezomodulated reflectivity[13,14,17,35–37] spectrum of sample 5 is compared in Fig. 4 to the numerical derivative of the reflectivity spectrum. Indeed, the piezoreflectivity, which is obtained by application of a small, alternating, biaxial strain in the plane of the samples, yields spectra proportional to the first derivative of the standard spectrum, but with amplitude coefficients which depend on the valence-band state involved (hh or lh). Due to the particular values of elastic constants and deformation potentials in ZnTe, lh exciton contributions are piezomodulated approximately three times more than those involving hh excitons. In Fig. 4, we have matched the amplitudes of both kinds of derivatives in the region of the ground (hh) excitonic transition. Then, all transitions for which both spectra are matched correspond to hh transitions. On the other hand, all instances where the piezomodulation gives stronger features correspond to lh excitons. This is shown by the labels in Fig. 4, where we have reproduced, for comparison, the direct reflectivity spectrum taken at $T=2$ K. Piezospectroscopy experiments are conducted at $T \sim 20$ K, which explains the small redshift of the whole spectrum, in this latter case, and the disappearance of excitonic complexes.

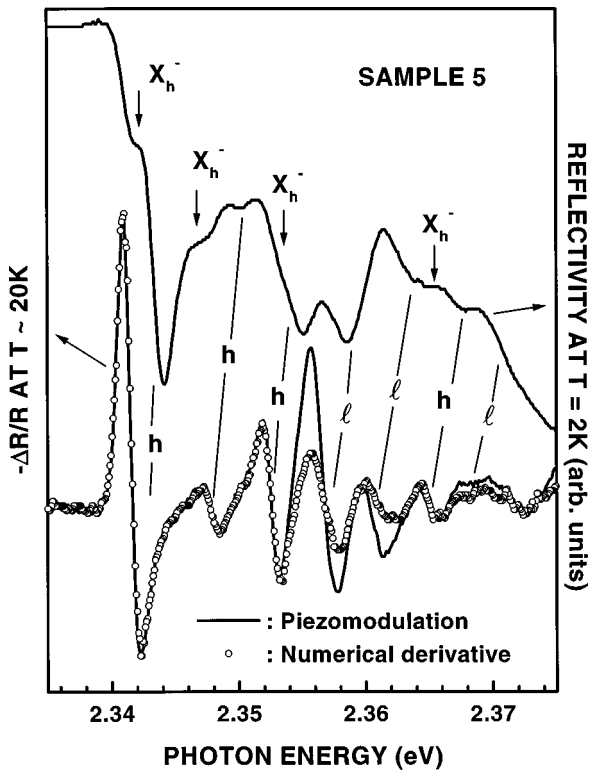

FIG. 4. Top: Reflectivity spectrum of sample 5, taken at $T=2$ K. All transitions labeled X_h^- are assigned to excitonic trions. Bottom: Numerical derivative (open dots) and piezomodulation (solid line) of the reflectivity, taken at $T \sim 20$ K (which explains the slight redshift). These spectra have been scaled so as to be matched in amplitude for the ground heavy-hole exciton transition. All resonances where the piezomodulation yields stronger features are assigned to light-hole exciton transitions.

The results in Fig. 4 demonstrate that we have a complex set of discrete, well-resolved, hh and lh contributions. These transitions cover the range between an energy close to that of the ground hh exciton of sample 1 and higher energies, closer to those of excitons in samples 2, 3, or 4. We interpret this observation as arising from five different configurations of CdTe islands in each of the five inserts, both in terms of island size and ordering and in terms of strain state. In other words, each pair of hh and lh exciton states corresponds to one of the five fractional CdTe inserts. There is no more possibility of resonant coupling between electronic states centered on each insert, as in sample 4, which would lead to the above-mentioned 3D superlattice state. Instead, we have different energy states, which remain coupled, however, as proved by the fact that the PL spectrum of sample 5 only reveals the fundamental hh exciton from one of the five inserts.

In fact, we wish to insist on the fact that the ground exciton in sample 5 almost lies *at the same energy* as that in

sample 1, while the inserts are half-ML instead of full ML. This comes in support of the idea that the only difference ''felt'' by excitons between sample 1 and sample 3 would be the strain state. In fact, we propose that the islands involved in the fundamental transition of sample 5 may be of comparable dimensions to those in sample 3, although they were expected to be smaller. But the additional uniaxial stress at the edges is relaxed in the case of *this insert* in sample 5. Consequently, the islands of this insert recover a strain state comparable to that of full ML in sample 1 and, thus, identical excitonic energies.

We believe that sample 5 exhibits a strong asymmetry along the growth axis, with the lowest exciton states corresponding to the insert on one side of the ZnTe well and the highest states to the insert on the other side. The progressive, steplike change of exciton energies between the different inserts could be due to a progressive change in the growth quality, due to the very low temperature. This would progressively change, in turn, the size and strain of the islands within each insert.

V. CONCLUSION

We have investigated in detail the effects of different deposition conditions on the optical properties of (sub)monolayer inserts of CdTe embedded in wide ZnTe/(Zn,Mg)Te quantum wells, grown on nominal (001) surfaces of ZnTe substrates. We have shown, in particular, that the ordering, size, and strain state of the monomolecular inserts are critically determined by the quality of the substrate and by the growth temperature. The energies and efficiencies of excitonic recombinations then depend also critically on growth conditions. Our results indicate that, at low temperature, ALE-grown islands (small ones) produce the most efficient luminescence, although they operate a rather shallow trapping of carriers (15 meV below the ground exciton of ZnTe). The latter characteristic may, however, have a decisive influence on the luminescence yield at higher temperatures, as indicated by preliminary results.[19]

Our results may delineate a few pathways for researchers who are currently trying to improve the emission characteristics of other Cd-based semiconductor objects of low dimensionalities, e.g., CdSe fractional layers in ZnSe or ZnMgSSe environments.

[1] Q. Xie, A. Madhukar, P. Chen, and N. P. Kobayashi, Phys. Rev. Lett. **75**, 2542 (1995).

[2] J. Y. Marzin, J. M. Gérard, A. Izrael, D. Barnier, and G. Bastard, Phys. Rev. Lett. **73**, 716 (1994).

[3] R. Engelhardt, V. Türck, U.-W. Pohl, and D. Bimberg, J. Cryst. Growth **184–185**, 311 (1998).

[4] J. L. Merz, S. Lee, and J. K. Furdyna, J. Cryst. Growth **184–185**, 228 (1998).

[5] P. D. Wang, N. N. Ledentsov, C. M. Sotomayor Torres, I. N. Yassievich, A. Pakhomov, A. Yu Egovov, P. S. Kop'ev, and V. M. Ustinov, Phys. Rev. B **50**, 1604 (1994).

[6] V. Bressler-Hill, A. Lorke, S. Varma, P. M. Petroff, K. Pond, and W. H. Weinberg, Phys. Rev. B **50**, 8479 (1994).

[7] W. Lei, Z. Wang, J. Liang, B. Xu, Z. Zhu, Z. Yuan, and J. Li, Appl. Phys. Lett. **67**, 1874 (1995).

[8] T. Utzmeier, G. Armelles, P. A. Postigo, and F. Briones, Phys. Rev. B **56**, 3621 (1997).

[9] N. N. Ledentsov, I. L. Krestinov, M. V. Maximov, S. V. Ivanov, S. L. Sorokin, P. S. Kop'ev, Zh. I. Alferov, D. Bimberg, and C. M. Sottomayor-Torres, Appl. Phys. Lett. **69**, 1343 (1996).

[10] A. A. Toropov, S. V. Ivanov, T. V. Shubina, A. V. Lebedev, S. V. Sorokin, P. S. Kop'ev, G. R. Pozina, J. P. Bergman, and B. Monemar, J. Cryst. Growth **184–185**, 293 (1998).

[11] N. Magnea, J. Cryst. Growth **138**, 550 (1994).

[12] Q. X. Zhao, N. Magnea, and J. L. Pautrat, Phys. Rev. B **52**, 16 612 (1995).

[13] V. Calvo, P. Lefebvre, J. Allègre, A. Bellabchara, H. Mathieu, Q. X. Zhao, and N. Magnea, Phys. Rev. B **53**, R16 164 (1996).

[14] P. Lefebvre, V. Calvo, N. Magnea, T. Taliercio, J. Allègre, and H. Mathieu, Phys. Rev. B **56**, 3907 (1997).

[15] I. L. Krestinov, M. V. Maximov, A. V. Sakharov, P. S. Kop'ev, Zh. I. Alferov, N. N. Ledentsov, D. Bimberg, and C. M. Sottomayor-Torres, J. Cryst. Growth **184–185**, 545 (1998).

[16] D. Martrou and N. Magnea, Proceedings of the E-MRS Spring Meeting (Symposium D), Strasbourg, France, 1998 [Mater. Sci. Eng. B (to be published)], and references therein.

[17] P. Lefebvre, V. Calvo, N. Magnea, T. Taliercio, J. Allègre, and H. Mathieu, Phys. Rev. B **56**, R10 040 (1997).

[18] N. Tomassini, A. D'Andrea, R. Del Sole, H. Tuffigo-Ulmer, and R. T. Cox, Phys. Rev. B **51**, 5005 (1995), and references cited therein.

[19] T. Taliercio, P. Lefebvre, N. Magnea, J. Allègre, and H. Mathieu, J. Cryst. Growth **184–185**, 844 (1998).

[20] K. Kheng, R. T. Cox, Y. Merle d'Aubigné, F. Bassani, K. Saminadayar, and S. Tatarenko, Phys. Rev. Lett. **71**, 1752 (1993).

[21] A. Naumov, D. Mi, M. D. Sturge, W. Ge, Le Si Dang, H. Mariette, and N. Magnea, J. Appl. Phys. **78**, 1196 (1995).

[22] K. Kheng, R. T. Cox, Y. Merle d'Aubigné, N. Magnea, H. Mariette, K. Saminadayar, and S. Tatarenko, Surf. Sci. **305**, 225 (1994).

[23] G. Finkelstein, H. Shtrinkman, and I. Bar-Joseph, Phys. Rev. Lett. **74**, 976 (1995).

[24] V. A. Shchukin, D. Bimberg, V. G. Malyshkin, and N. N. Ledentsov, Phys. Rev. B **57**, 12 262 (1998).

[25] J. M. Hartmann, G. Feuillet, M. Charleux, and H. Mariette, J. Appl. Phys. **79**, 3035 (1996).

[26] J. M. Hartmann, J. Cibert, F. Kany, H. Mariette, M. Charleux, P. Alleysson, R. Langer, and G. Feuillet, J. Appl. Phys. **80**, 6257 (1996).

[27] D. Brinkmann and G. Fishman, Phys. Rev. B **56**, 15 211 (1997).

[28] T. Richard, P. Lefebvre, H. Mathieu, and J. Allègre, Phys. Rev. B **53**, 7287 (1996).

[29] P. Lefebvre, T. Richard, H. Mathieu, and J. Allègre, Solid State Commun. **98**, 303 (1996); **100**, 547 (1996).

[30] Ph. Lelong and G. Bastard, Solid State Commun. **98**, 819 (1996), and references therein.

[31] Huaxiang Fu and A. Zunger, Phys. Rev. B **56**, 1496 (1997), and references therein.

[32] A. Franceschetti and A. Zunger, Phys. Rev. Lett. **78**, 915 (1997).

[33] G. Allan, C. Delerue, and M. Lannoo, Phys. Rev. Lett. **76**, 2961 (1996).
[34] G. L. Bir and G. E. Pikus, in *Symmetry and Strain Induced Effects in Semiconductors* (Wiley, New York, 1974).
[35] H. Mathieu, P. Lefebvre, J. Allègre, B. Gil, and A. Regreny, Phys. Rev. B **36**, 6581 (1987).
[36] H. Mathieu, J. Allègre, and B. Gil, Phys. Rev. B **43**, 2218 (1991).
[37] J. Calatayud, J. Allègre, P. Lefebvre, and H. Mathieu, Mater. Sci. Eng. B **16**, 87 (1993).